



Formulation and Characterization of Nystatin-loaded Nanostructured Lipid Carriers for Topical Delivery against Cutaneous Candidiasis

**Rawia M. Khalil^{1*}, A. Abd- Elbary², Mahfouz A. Kassem¹,
Mohamed S. El Ridy¹, Mona M. Abou Samra¹, Ghada E. A. Awad³
and Soheir S. Mansy⁴**

¹Department of Pharmaceutical Technology, National Research Centre, Dokki, CAiro, Egypt.

²Faculty of Pharmacy, Cairo University, Cairo, Egypt.

³Chemistry of Natural and Microbial Product Department, National Research Centre, Dokki, Cairo, Egypt.

⁴Electron Microscopy Research department Theodor bilharz Research Institute, Cairo, Egypt.

Authors' contributions

This work was carried out in collaboration between all authors. Author RMK designed the study, wrote the protocol, managed the analyses of the study and reviewed the manuscript. Author MMAS carried out the experimental work, performed the statistical analysis and wrote the first draft of the manuscript. Authors MAK, AAE and MSER checked the revised manuscript thoroughly and confirmed all the data given in manuscript and managed the literature. Author GEAA carried out the microbiological experiments. Author SSM performed the histopathologic examinations and the discussion of the pathological findings. All authors read and approved the final manuscript.

Original Research Article

Received 23rd September 2013

Accepted 29th November 2013

Published 24th December 2013

ABSTRACT

Aims: The objective of the current study was to formulate nystatin (Nyst) into nanostructured lipid carriers (NLCs) to enhance its antifungal activity.

Place and Duration of Study: Department of pharmaceutical technology, national research centre, Egypt, between mars 2011 to april 2013

Methodology: Nyst loaded NLCs (NYST-NLCs) were prepared by the hot homogenization and ultrasonication method followed by evaluation of its topical effect on

*Corresponding author: Email: rawia_khalil@yahoo.com;

the cutaneous candidiasis. The prepared Nyst-NLCs were characterized for entrapment efficiency, particle size, zeta potential, morphology (transmission electron microscopy), thermal characterisation (differential scanning calorimetry) and in vitro drug release. The study design involves the investigation of the effect of three independent variables namely liquid lipid type (Miglyol 812 and Squalene), liquid lipid concentration (30 and 50%) and Nyst concentration (0.125 and 0.25%). A stability study for 6 months was performed. A microbiological study was conducted in male rats infected with *Candida albicans*.

Results: NLC dispersions were spherical in shape with particle size ranging from 68.06 ± 6.56 to 141.8 ± 3.33 nm. The entrapment efficiencies ranged from 45.50 ± 2.34 to $92.73 \pm 0.33\%$ with zeta potential ranging from -26.2 to -39.2 mV. The stability studies done for 6 months indicated that Nyst-NLCs were stable for more than 6 months. The microbiological studies showed A least number of colonies forming units (cfu/ml) were recorded for the selected Nyst-NLCs compared to the drug solution and the Nystatin® cream present in the market.

Conclusion: It can be fulfilled from this work that NLCs represent promising carrier for topical delivery of Nyst offering good physical stability, high entrapment efficiency and controlled drug release. Nyst-NLCs are a good candidate for cutaneous treatment of fungal infection.

Keywords: Nanostructured lipid carriers; characterization; Nystatin; fungal infection; *Candida albicans*.

1. INTRODUCTION

Solid lipid nanoparticles (SLNs) combining the advantages of colloidal carriers, had attracted attention as a drug delivery system when it was introduced in 1991 [1]. Several advantages of SLNs including biocompatibility, drug targeting, modified release and ease of large scale production have been demonstrated [2]. However, depending on the drug, some potential problems can occur, such as drug leakage during storage and insufficient total drug loading. To overcome the limitations of SLNs, nanostructured lipid carriers (NLCs) have been developed [3]. NLCs are produced by mixing the solid lipid with the liquid lipid. This leads to special nanostructures with improved properties for drug loading, modulation of the drug release profile and stability [3,4]. Nystatin (Nyst) is a polyene antibiotic produced by *Streptomyces noursei*; used topically in treatment of infections due to *Candida albicans*, *Aspergillus* species, yeasts and some dermatophytes. It is often used in large doses which vary from 100,000 units (for oral infections) to 1 million (for intestinal ones) at risk of fungal infections such as AIDS patients and patients receiving chemotherapy. Trials to improve the effectiveness of Nyst or decrease its dose are ongoing. Recently, topical formulation of nystatin was developed, Quinones et al, prepared a Nyst gel for topical delivery [5]. Melkoumov et al. succeeded to prepare Nyst nanosuspension by wet media milling [6]. Other researches were done to study the effect of silver nanoparticles in combination with Nyst against *candida albicans* [7,8]. The aim of the current study is to develop lipid nanoparticulate formulations of Nyst in an attempt to increase its efficacy for topical application. Its formulation in nanostructured lipid carriers may promote its lethal effect as its mode of action depends on its binding to ergosterol, a major component of the fungal cell membrane forming pores in the membrane that lead to potassium leakage and death of the fungus.

2. MATERIALS AND METHODS

2.1 Materials

Nystatin, kindly supplied by Ramedia Pharmaceuticals, Sixth of October, Egypt. Compritol 888 ATO (glyceryl behenate), kindly donated by Gattefossé, France. Nystatin[®] cream purchased from the Egyptian market. Poloxamer 188 (Pluronic F68; a triblock copolymer of polyoxyethylene- polyoxypropylene), PVA (polyvinyl alcohol), Dialysis tubing cellulose membrane (molecular weight cut-off 12,000-14,000 g/mole) and Methanol were purchased from Sigma-Aldrich Chemical Company., St.louis, USA. Miglyol 812 and Squalene were purchased from Sigma-Aldrich Chemical Company., St.louis, USA. Potassium dihydrogen orthophosphate and citric acid were of analytical grade.

2.2 Methods

2.2.1 Formulation technique

Nanostructured lipid carriers were prepared by the modified high shear homogenization and ultrasonication method [9,10,11]. The lipid was melted to approximately 5°C above its melting point (74.09°C), replacing 30 %w/w and 50%w/w of the solid lipid matrix by Miglyol[®] 812 or Squalene (liquid lipid). Nyst was dispersed in the melted Compritol 888 ATO. An aqueous phase was prepared by dissolving the surfactant (poloxamer 188 or PVA) in distilled water and heating up to the same temperature of the molten lipid. The hot lipid phase was poured on the aqueous phase and homogenization was carried out at 25000 rpm for 5 minutes using Heidolph homogenizer. The resulted O/W emulsion was sonicated for 30 minutes (water bath sonicator). The dispersion thus obtained was allowed to cool to room temperature, forming lipid nanoparticles by recrystallization of the dispersed lipid [12]. The produced Nyst-NLCs were kept at 4°C for 24 hours before centrifugation at 9000 rpm for 30 minutes and separation. Different formulations are presented in Tables 1 and 2.

Table 1. Composition of Nyst-NLCs using Miglyol 812[®] as liquid lipid

Formulations	Surfactants		Lipid conc.		Drug conc. (w/w)
	Type	Conc. (%w/w)	Compritol	Miglyol	
NLC1		1	70	30	0.25
NLC2		1	50	50	0.25
NLC3	Poloxamer 188	2.5	70	30	0.125
NLC4		2.5	50	50	0.125
NLC5		2.5	70	30	0.25
NLC6		2.5	50	50	0.25
NLC7		5	70	30	0.25
NLC8		5	50	50	0.25
NLC9		1	70	30	0.25
NLC10		1	50	50	0.25
NLC11	PVA	2.5	70	30	0.125
NLC12		2.5	50	50	0.125
NLC13		2.5	70	30	0.25
NLC14		2.5	50	50	0.25
NLC15		5	70	30	0.25
NLC16		5	50	50	0.25

Table 2. Composition of Nyst-NLCs using Squalene as liquid lipid.

Formulations	Surfactants		Lipid conc.		Drug conc. (w/w)
	Type	Conc. (%w/w)	Compritol	Miglyol	
NLC17	Poloxamer 188	1	70	30	0.25
NLC18		1	50	50	0.25
NLC19		2.5	70	30	0.125
NLC20		2.5	50	50	0.125
NLC21		2.5	70	30	0.25
NLC22		2.5	50	50	0.25
NLC23		5	70	30	0.25
NLC24		5	50	50	0.25
NLC25		1	70	30	0.25
NLC26		1	50	50	0.25
NLC27	PVA	2.5	70	30	0.125
NLC28		2.5	50	50	0.125
NLC29		2.5	70	30	0.25
NLC30		2.5	50	50	0.25
NLC31		5	70	30	0.25
NLC31		5	50	50	0.25

2.2.2 Characterization

2.2.2.1 Particle size and zeta potential measurements

Size and zeta potential of NLCs were measured using a Zetasizer (Nano ZS) at 25°C. Samples were diluted appropriately with the aqueous phase of the formulation for the measurements.

2.2.2.2 Entrapment efficiency determination

The entrapment efficiency was determined indirectly by measuring the concentration of the drug in the supernatant after centrifugation. The untrapped nystatin was determined by adding 1ml of Nyst-NLCs to 9 ml methanol and then this dispersion was centrifuged at 9000 rpm for 30 minutes at -4°C, and then washed 3 times with methanol. The supernatant was collected, filtered through millipore membrane filter (0.2µm) then diluted with methanol and measured spectrophotometrically at λ=303.8 nm. The entrapment efficiency (E.E) was calculated using the following equation [13,14]:

$$E.E\% = \frac{W \text{ initial drug} - W \text{ free drug}}{W \text{ initial drug}} \times 100$$

Where “W initial drug” is the mass of initial drug used and the “W free drug” is the mass of free drug detected in the supernatant after centrifugation of the aqueous dispersion.

2.2.2.3 Transmission electron microscopy (TEM)

Morphology of the selected NLCs was examined by TEM. One drop of diluted sample was stained with 2% (W/V) phosphotungstic acid for 30 seconds and then placed on copper grids with films for viewing.

2.2.2.4 Differential scanning calorimetry (DSC)

The thermal characteristics of selected batches of lipid nanoparticles were determined by differential scanning calorimetry (DSC)-50, Kyoto, Japan. Samples containing 10 mg nanoparticle dispersions were weighed accurately into standard aluminium pans using an empty pan as a reference. DSC scans were recorded at a heating and cooling rate of 10°C/min. The samples were heated from 30-300°C and cooled from 300-30°C.

2.2.3 Drug release study

The in-vitro release of Nyst from different NLCs was evaluated by the dialysis bag diffusion technique reported by Yang et al. [15]. The release studies of Nyst from lipid nanoparticles were performed in phosphate buffer of pH 5.5 and methanol (70:30). The nanostructured lipid carriers of Nyst equivalent to 2 mg of Nyst were suspended in the buffer solution (pH 5.5) and placed in a dialysis bag (donor compartment) and sealed at both ends. The dialysis bag was immersed in the receptor compartment containing 50 ml of the dissolution medium, which was stirred at 100 rpm and maintained at 32±2°C. The receptor compartment was covered to prevent evaporation of the dissolution medium. Samples (2 ml) were taken from the receptor compartment and the same amount of fresh dissolution medium was added to keep a constant volume at fixed time intervals (0.5, 1, 2, 3, 4, 5, 6, 7, 8 and 24 h). Nyst in the samples was measured spectrophotometrically at $\lambda=303.8$ nm. The release studies were carried out in triplicate for all formulations and the results were expressed as the mean values ±SD.

2.2.4 Stability study

The selected NLC formulations were stored in a sealed amber colored glass vials at refrigerator temperature (2-4°C) in a dark environment. The physical appearance was assessed and the formulations were analyzed with respect to particle size, drug entrapment efficiency and zeta potential after 6 months of storage and compared with fresh formulations. In addition, the drug release properties of the Nyst-NLCs stored for 6 months were evaluated and compared with those of fresh formulations. The experiment was performed in triplicate. Shelf life values were calculated as follows [16]:

The values of Log E.E. % were plotted against the time (days of storage) and the slopes (m) were calculated by linear regression. The slopes (m) were then substituted into the following equation for the determination of K values [17]:

$$K = m \times 2.303.$$

As reported by Wells [18], the shelf life values (the time for 10% loss, t_{90}) were then calculated by the following equation:

$$t_{90} = 0.105/K.$$

2.2.5 Antifungal activity

2.2.5.1 Preparation of the animals

Male albino rats (120-150g) purchased from the animal house of the National Research Centre were used in the experiment. These rats were divided into five groups; six animals were used for each group. Group 1 served as control, group 2 was treated with the plain drug solution, group 3 received topically an equivalent dose of Nystatin[®] cream present in the market and group 4 and 5 received topically the NLC3 and NLC27 formulae respectively. The rats were housed in individual cages and received food and water ad libitum. The experimental protocol of the study was reviewed and approved by the Animal Ethics Committee of the National Research Centre. Experiments were carried out in accordance with the guidelines laid down by the National Research Centre regarding the care and use of animals for experimental procedures and in accordance with local laws and regulations.

2.2.5.2 Preparation of microorganism

Clinical isolate of *Candida albicans* was used to infect the animals. A working culture of *Candida* was grown for 24 h at 37°C on Potato Dextrose Broth (PDB). The culture was diluted with a sterile saline solution to reach a final concentration of 1.1×10^6 colony forming unit/ ml (cfu/ml) according to the modified method of Maebashi et al. [19].

2.2.5.3 Cutaneous infection

Each animal's back was shaved; approximately 5.0cm² area was marked on each animal's back. The marked area was infected with 1.1×10^6 cfu/ml suspension by gently rubbing onto the skin with the help of a sterile cotton-tipped swab until no more visible fluid was observed [19]. Infection was produced under an occlusive dressing and the infected area was covered with a sterile adhesive bandage, held in place with extra-adherent tape for 24h before treatment began. Control animals were infected in the same manner; however, they did not receive any Nyst formulation.

2.2.5.4 Treatment of the infection

Treatment began 24h after the infection was induced, and test formulations were topically applied twice daily for two consecutive days. After 48 h of treatment swabs were taken from each infected area into sterile tubes containing 5 ml of (PDB). Serial dilutions were done and then one ml of each dilution was inoculated into Petri dishes containing 10 ml of Potato Dextrose Agar (PDA). The inoculated plates were incubated for 24h at 37°C after which the colonies were counted.

2.2.5.5 Histopathological examination

After taking the skin swab in a way the skin is completely cleaned out from the infected organism, the rats are sacrificed. The defined part of the shaved skin is excised and fixed in 10% formalin. The fixed skin tissues were processed until embedded in paraffin [20]. Two sections of 4µm thickness were performed from each skin embedded in paraffin block using microtome. One section was stained with Haematoxylin and eosin as well as the other was stained with Masson trichrome [20].

2.2.6 Stastical analysis

All the results were expressed as mean±S.D. Statistical analysis of the results was performed using SPSS program with help of one way analysis of variance (ANOVA), followed by post hoc multiple comparisons and least significant difference (LSD). The results are significant when $P < 0.05$.

3. RESULTS AND DISCUSSION

In this study, Compritol as solid lipid (5%), Miglyol 812 or squalene as liquid lipid (30 and 50%), Poloxamer 188 or PVA as stabilizers (1%, 2.5% and 5%) and Nyst (0.125 and 0.25%) were used to produce NLCs (Table1&2).

3.1 Characterization of the Prepared Nyst-NLCs

3.1.1 Particle size analysis

Table 3 shows the effect of increasing Miglyol® 812 or Squalene percentage in the lipid matrix from 30% to 50% with constant surfactant concentration at 2.5 %w/w and constant drug concentration at 0.25%w/w. The results show that increasing the concentration of liquid lipid is accompanied with a decrease in particle size. Based upon previous studies; the addition of Miglyol® 812 to Compritol tends to promote the formation of small particle population, which might be due to a higher molecular mobility of the matrix after liquid oil addition [21,22]. Also, the effect of oil content on particle size was in agreement with the work performed by Chen et al. who found that increasing the concentration of Squalene to Precirol from 0-80% resulted in significant decrease in particle size from 286.5±3.7 nm to 210.4±5.6 nm [23]. Similar observation was reported by Khalil et al. [24] who found that increasing Miglyol concentration in meloxicam NLCs resulted in a significant decrease in particle size.

The drug concentration has also a marked role on the particle size. The results show that the particle size increases with increasing drug concentration from 0.125 %(w/w) to 0.25%(w/w) (Table 4). This can be explained as the lipid has a certain loading capacity, the addition of excess drug may lead to aggregation and the formation of large sized particles [25]. Considering the effect of surfactants on the particle size of different Nyst-NLCs, it was noticed that the change in surfactant types and concentrations doesn't show a remarkable effect.

3.1.2 Entrapment efficiency (E.E)

The entrapment efficiency of Nyst within the different prepared nanostructured lipid carrier formulaions is shown in Tables 3 and 4 and Figs. 1 and 2. Increasing surfactant concentrations from 1 to 5% w/w was accompanied with increase in the E.E%, (NLC2, NLC6 & NLC8) and (NLC10, NLC14 & NLC16) for poloxamer 188 and PVA respectively (Figs. 1 and 2). This might be due to the efficient loading and retention of drug molecules within the nanoparticle matrix or nanoparticle surface at higher surfactant concentration [22]. Concerning the effect of surfactant type, it was noticed that the effect of PVA is higher than poloxamer 188 on the entrapment efficiencies. This increase in the E.E% may be also due to the increase in the solubility of the drug in the lipid on increasing the concentration of the surfactant [26,27]. The results reveal that replacing solid lipid by increasing percent of liquid

lipid leads to a gradual increase in E.E% (Table 3). In general, drug solubility is higher in liquid lipid than in solid lipid, which increases the E.E% [28]. Incorporation of liquid lipids into solid lipids leads to massive crystal order disturbance. Greater imperfections in the crystal lattice leave enough space to hold drug molecules, which ultimately improved drug loading capacity and drug entrapment efficiency [29]. Increasing the amount of drug, while keeping the emulsifier level constant, as shown in table 4 is found to decrease the E.E%. As the lipid has certain drug loading capacity, addition of excess drug led to increase of unencapsulated -drug (i.e. decrease in E.E.%), which signifies that E.E.% reaches its maximum at 0.125% drug concentration [25].

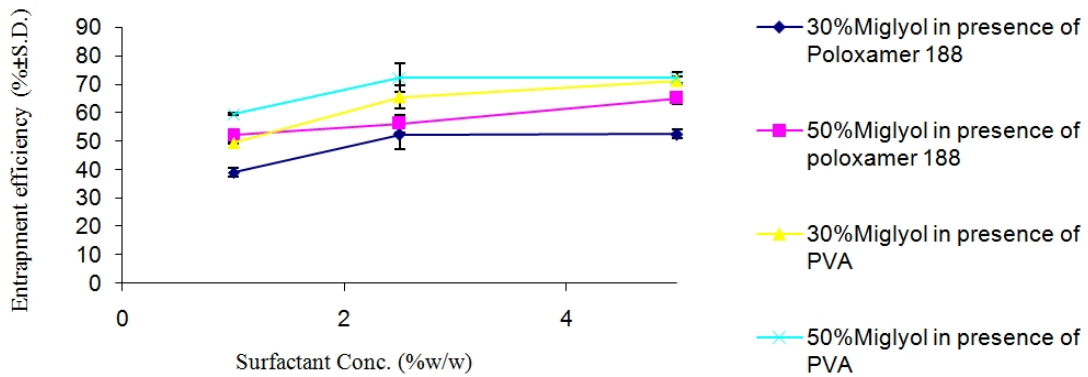


Fig. 1. Effect of type and concentration of surfactants on the entrapment efficiency of Nyst-NLCs in presence of Miglyol

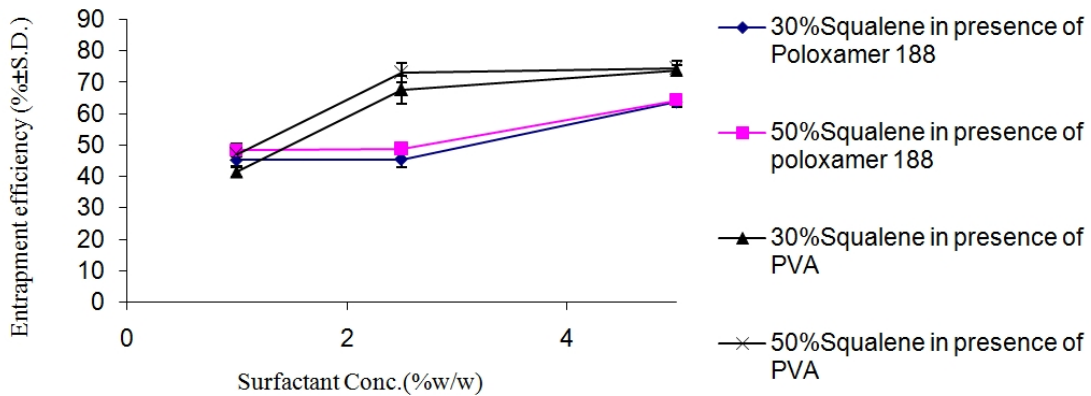


Fig. 2. Effect of type and concentration of surfactants on the entrapment efficiency of Nyst-NLCs in presence of Squalene

Table 3. Effect of liquid lipid on the entrapment efficiency and the particle size of Nyst-NLCs

Formulae	Surfactant		Lipid Conc.(%w/w)			Drug Conc. (%w/w)	Entrapment efficiency (%±S.D.)	Particle size (nm±S.D.)
	Type	Conc. (%w/w)	Compritol	Miglyol	Squalene			
NLC5			70	30	-		52.43±5.04	141.8±2.33
NLC6			50	50	-		56.05±3.04	122.4±6.47
NLC21	Poloxamer 188		70	-	30		45.50±2.34	105.7±5.12
NLC22			50	-	50		48.93±0.96	105.7±2.45
NLC13		2.5	70	30	-	0.25	65.46±4.05	105.7±2.22
NLC14			50	50	-		72.20±5.12	91.28±9.52
NLC29	PVA		70	-	30		67.73±4.52	105.7±8.22
NLC30			50	-	50		73.20±3.11	91.28±6.53

Table 4. Effect of drug concentrations on the entrapment efficiency and the particle size of Nyst-NLCs

Formulations	Surfactant		Drug Conc.(%w/w)	Entrapment efficiency (%±S.D.)	Particle size (nm±S.D.)
	Type	Conc.(%w/w)			
NLC3				85.86±0.45	68.06±6.56
NLC4			0.125	92.73±0.33	78.82±11.22
NLC19				61.34±1.45	91.82±6.53
NLC20	Poloxamer 188			66.40±1.55	58.77±3.58
NLC5					52.30±5.04
NLC6			0.25	56.05±3.04	122.4±6.47
NLC21				45.50±2.34	105.7±5.12
NLC22				48.93±0.96	105.7±2.45
NLC11		2.5		69.46±1.01	105.7±2.22
NLC12			0.125	72.20±0.77	91.28±9.52
NLC27				72.20±2.11	105.7±8.22
NLC28	PVA			78.40±0.75	91.28±6.53
NLC13					65.46±4.05
NLC14			0.25	72.20±5.12	102.5±2.56
NLC29				67.73±4.52	141.8±3.33
NLC30				73.20±3.11	105.7±5.12

3.1.3 Zeta potential

All formulations were negatively charged with zeta potential values ranging from -23.2 to -39.2 mV for NLC10 & NLC9 respectively indicating a relatively good stability and dispersion quality. It is noticeable that increasing the surfactant concentration in the formulation does not affect the zeta potential.

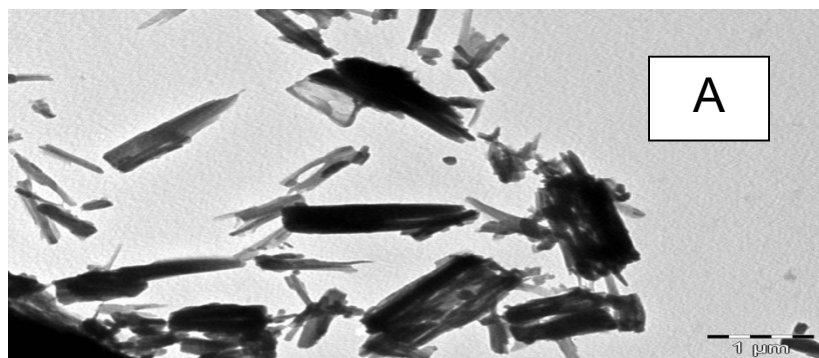
Concerning the effect of the drug concentration on the zeta potential, it is noticed that the absolute values of zeta potential decrease as the amount of drug added increase especially in case of poloxamer 188 with Miglyol®812 (Table 5). The larger particle size obtained upon increasing the drug concentration led to lower charge density of particle and absolute values of zeta potential [30]. However, no linear correlation between the zeta potential and liquid lipid concentration was observed. This was in agreement with Chen et al. who observed that different Squalene ratios did not affect the zeta potential of the prepared NLCs [23].

Table 5. Effect of drug concentrations on the zeta potential values of Nyst-NLCs

Formulations	Surfactant		Lipid		Drug Conc. (%w/w)	Zeta potential (mv)
	Type	Conc. (%w/w)	Type	Conc. (%w/w)		
NLC3					30	-33.4
NLC4					50	-32.2
NLC5	Poloxamer 188	2.5	Miglyol® 812		30	-26.6
NLC6					50	-23.6
NLC11					30	-31.1
NLC12					50	-32.2
NLC13	PVA		Squalene		30	-31.2
NLC14					50	-32.8

3.1.4 Transmission electron microscopy (TEM)

Fig. 3(A) shows the TEM micrograph of Nyst which appears as needles like crystalline shape. The morphology of NLC dispersions was investigated and presented in Fig. 3. The TEM micrographs revealed an almost spherical shape of the particles irrespective of the oil load. It can be noticed that the most important result of the electron microscopic study is the absence of clearly identifiable oil droplets in the NLC samples which may result from separated oil phase in these samples, i.e. at a Miglyol®812 and Squalene load of 30-50% no phase separation was observed.



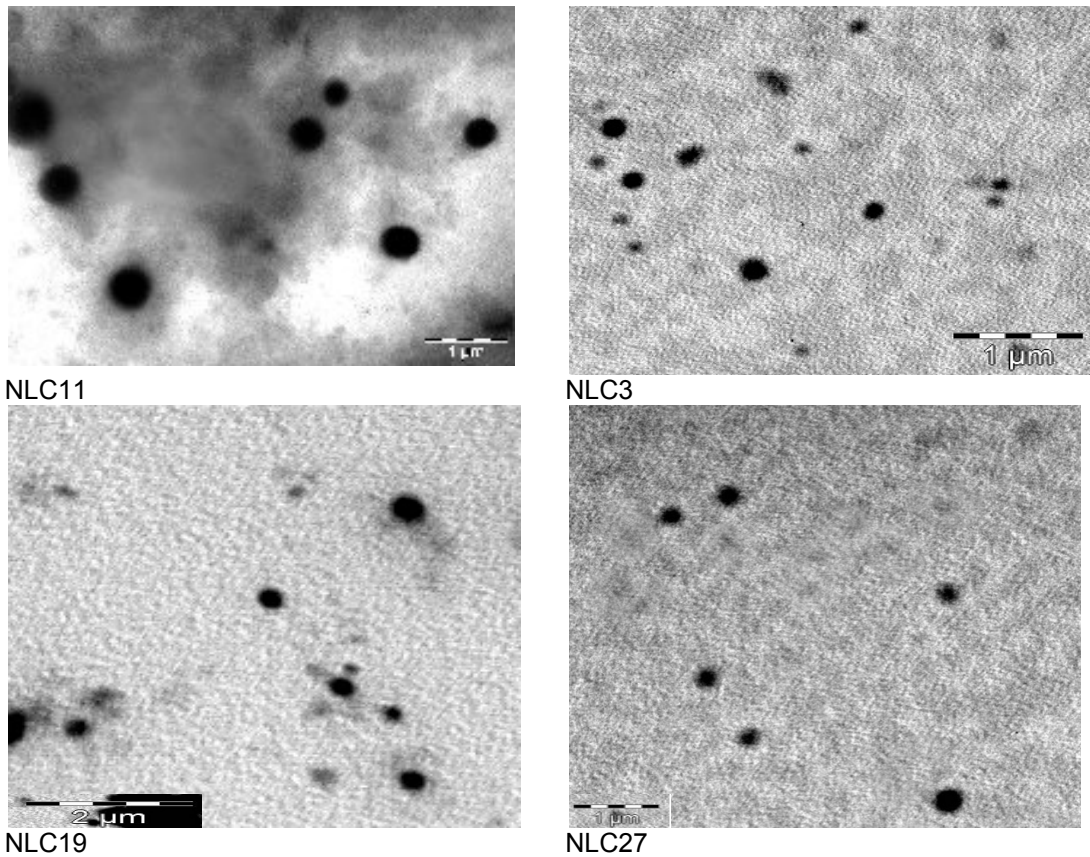


Fig. 3. Transmission electron micrographs of free Nyst (A) & micrograph of different Nyst-NLCs formulations

3.1.5 Differential scanning calorimetry

The DSC data of Nyst, bulk lipid and Nyst- NLCs are presented in figure 4. Nystatin and compritol showed sharp endothermic peaks at 167.11°C and 74.09°C, respectively. Miglyol ®812 and Squalene were not examined by DSC because liquids cannot be registered using the described temperatures and analytical conditions. The data clearly show that the melting endothermic of Nyst (167.11 °C) was not recorded indicating the complete solubilization of Nyst in the lipid matrix. It was noticed that the addition of a liquid lipid (Miglyol ®812 or Squalene) to solid lipid (compritol) induced a shift of the melting point to lower temperatures from 74.09 to 66.84°C, 66.92°C, 67.32°C and 68.31°C in case of NLC3, NLC11, NLC19 and NLC27, respectively. A sharp reduction in melting enthalpy (required to melt the lipid matrix) indicates an interaction of liquid oil with the crystalline lipid matrix, creating a more massive crystal order disturbance (lattice defects) which could allow enough space to accommodate Nyst molecules [31].

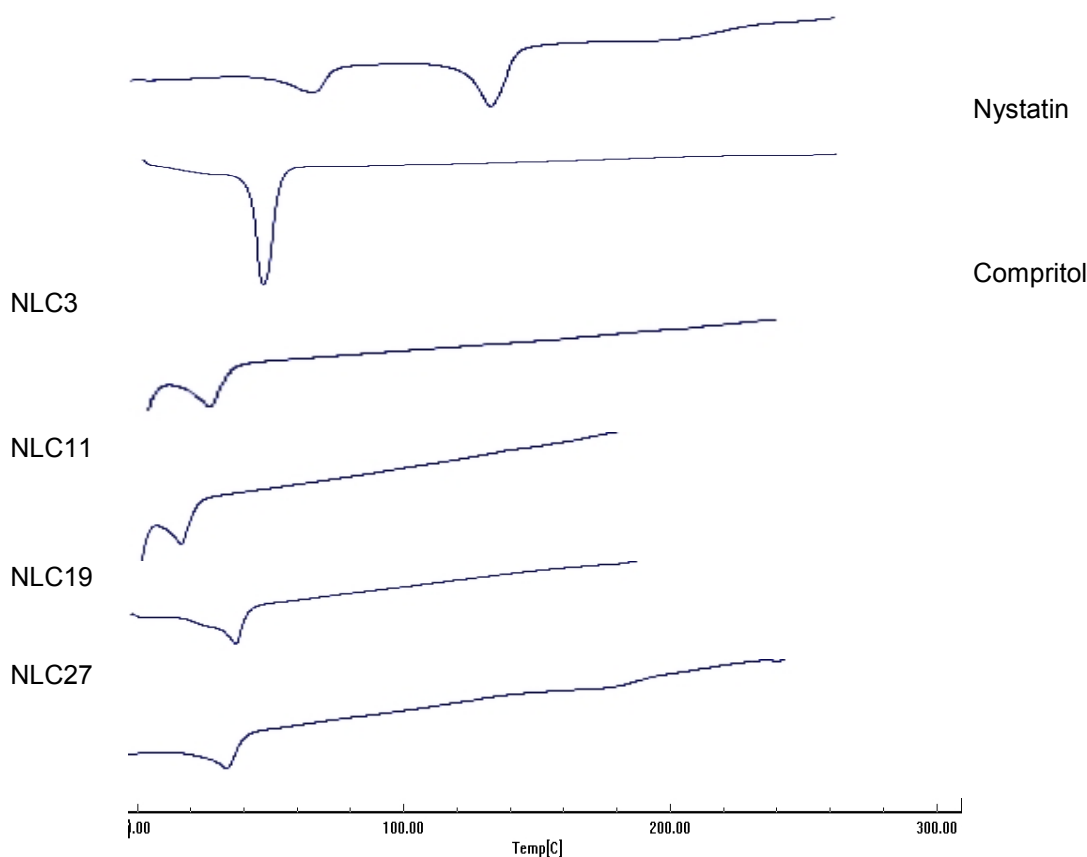


Fig. 4. DSC thermograms of pure Nyst, compritol and different Nyst-NLCs formulations.

3.2 Drug Release Study

Figure 5 shows the effect of lipid concentration when using 2.5%w/w of different surfactants and 0.25%w/w of the drug. The increase in the oil concentration from 30%w/w to 50%w/w of the lipid is accompanied with a decrease of the percentage of Nyst released. All the formulae in which 50% of the lipid was replaced by Miglyol or Squalene show the lowest percent of drug released compared to the formulae containing 30% of the liquid oil. This may be due to that increasing the oil concentration may lead to increase in the viscosity of the system leading to suppression of the release. Another reason, that after lipid crystallization, the solubility of oil in solid lipid exceeded; hence, oil precipitates leading to formation of fine droplets of oil incorporated in solid lipid thereby providing prolonged release [32]. The results also pointed to the effect of drug concentration on the release of Nyst from NLCs release profile. Figs. 6 and 7 show that upon increasing the drug concentration from 0.125%w/w to 0.25% w/w there is a significant decrease in the percentage released of Nyst from NLCs formulations.

As discussed before, Nyst is released more quickly when used in lower concentration because of the drug-enriched shell model [33,34]. The release data are analyzed according

to zero, first order and Higuchi equations which are widely used in determining the release kinetics of lipid nanoparticles. The amount of Nyst released from all the NLCs formulations studied shows a linear relationship with the square root of time, therefore, the release rate of Nyst is expressed following the theoretical model by Higuchi [35].

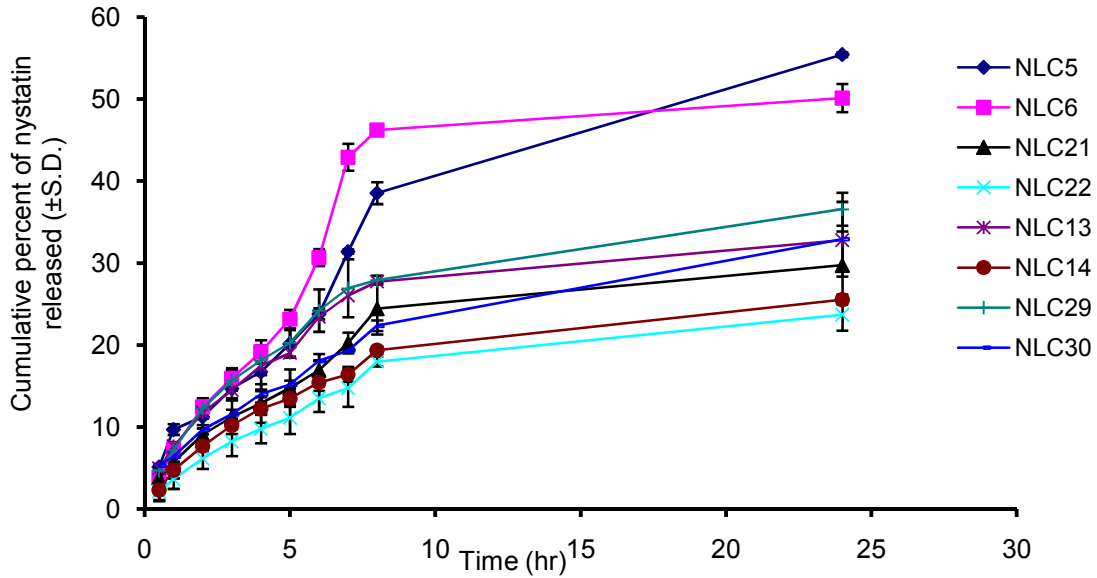


Fig. 5. Effect of liquid lipid on the in vitro release of Nyst from NLCs

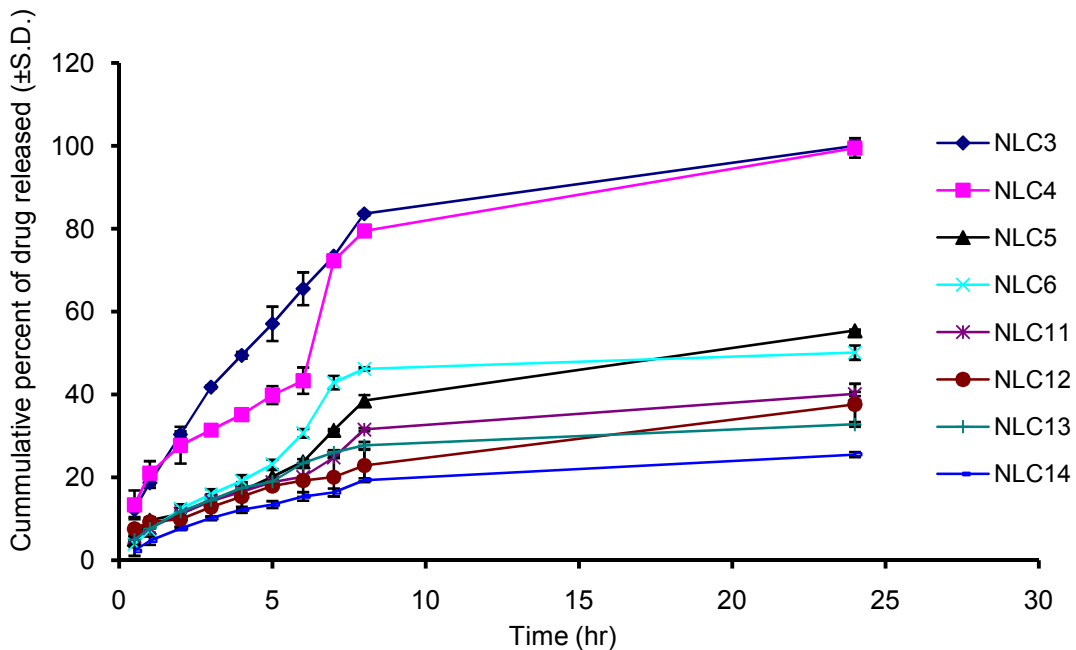


Fig. 6. Effect of drug concentration on the in-vitro release of Nyst from NLCs in presence of Miglyol.

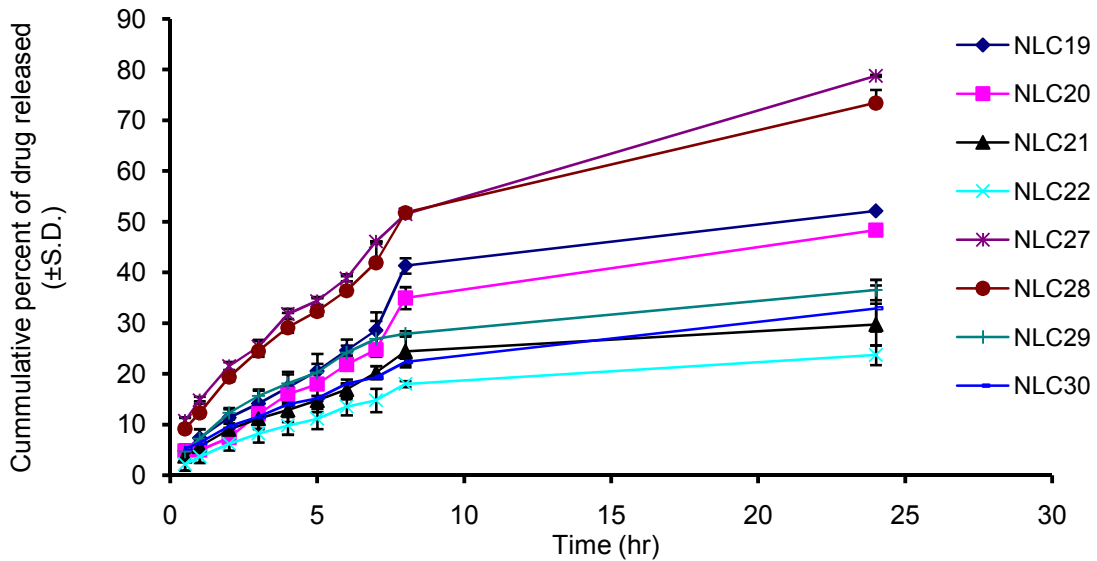


Fig. 7. Effect of drug concentration on the in-vitro release of Nyst from NLCs in presence of Squalene

3.3 Stability Study

Stability was performed for 2 formulations which are, NLC3 and NLC27 as they show the highest cumulative percent of Nyst released. The physical stability of Miglyol 812 and Squalene NLCs formulations was suggested by the absence of visible phase separation and all dispersions remained in a homogenous state upon storage at 2-4°C for 6 months. The mean of the entrapment efficiency and particle size of the prepared NLCs after storage are shown in Figs. 8 and 9. A non significant increase was observed in the entrapment efficiency and the particle size for the stored samples. Fig. 10 shows the values of the zeta potential which decrease with time but still indicating stability of the formulations. The in-vitro release profile of Nyst from the nanostructured lipid carriers (NLC3 & NLC27) was investigated over 24 h. The results are shown in Fig. 11. The drug release rate of NLC 3 & NLC27 after 2, 4 & 6 months shows no significant increase compared to freshly prepared ones. The t90 values for NLC3 and NLC27 were eleven and eight months respectively. In this respect it can be hypothesized that the stability of Nyst is better controlled in NLC3.

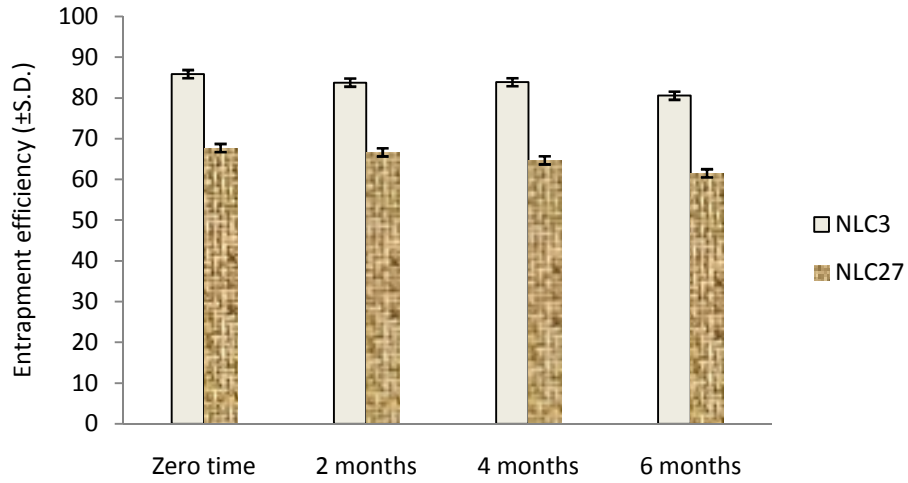


Fig. 8. Effect of storage time on the entrapment efficiency of different Nyst –NLCs

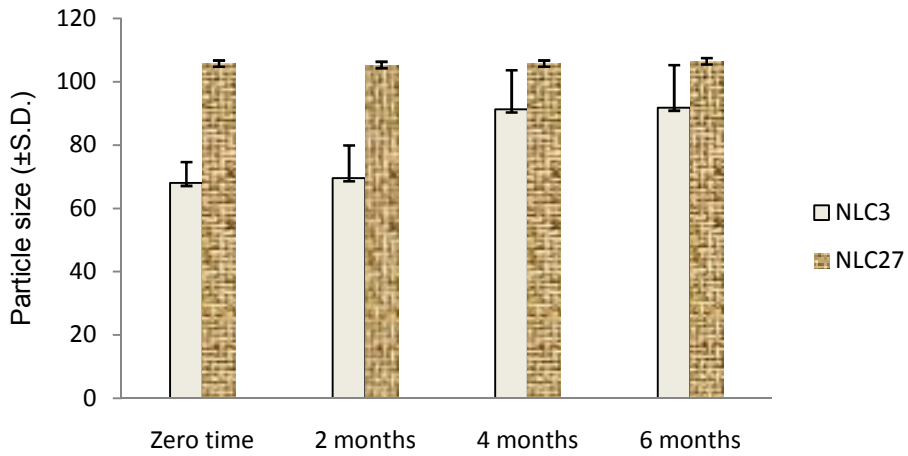


Fig. 9. Effect of storage time on the particle size of different Nyst-NLCs

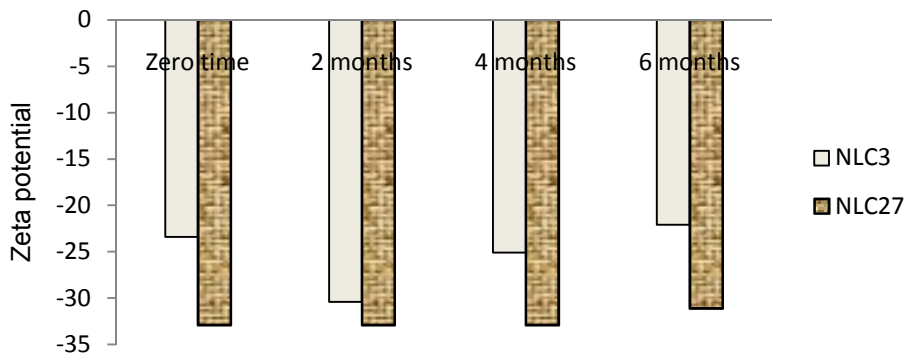


Fig. 10. Effect of storage time on the zeta potential of different Nyst-NLCs

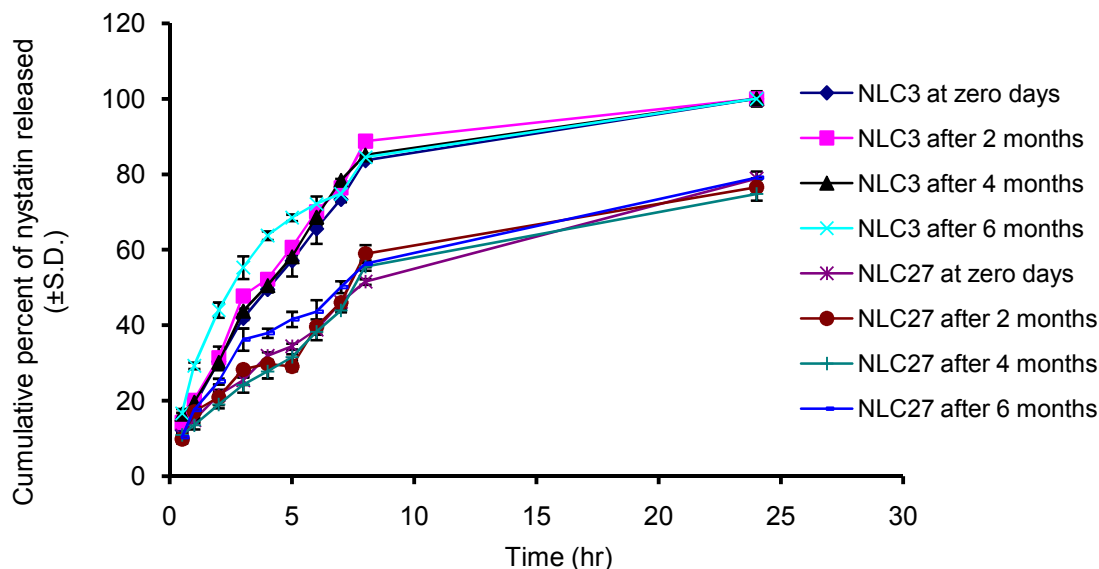


Fig. 11. Effect of storage time on the in-vitro release of Nyst from NLCs.

3.4 Antifungal Activity

After two days of treatment with plain drug solution, Nystatin[®] cream and the tested formulae (NLC3 and NLC27), the animals treated with the tested formulae demonstrated a low colony count significantly ($p < 0.05$) less than that for those animals treated with plain drug solution and Nystatin[®] cream (Fig. 12). The higher therapeutic efficacy in the case of NLC formulations may be expected due to penetration into the skin, followed by drug carrier accumulation in different strata of the skin resulting a reservoir effect with higher level of localization [36,37]. These findings also confirmed that lipid nanoparticles provoke the accumulation of the embedded drug into the upper skin layers [38].

It is clear from the histopathology (Figs. 13-18) of the skin biopsies stained with Masson trichrome & Haematoxylin and eosin that the skin of the normal control rat reveals keratinized squamous epithelium with intact basal cell layer and basal lamina. The basal part of the epidermis is folded to form the dermal papillae. Hair follicles were clearly identified with their different constituents extending into the dermis. The dermis formed the thick connective tissue layer in which the hair follicles were seen with sebaceous glands. This histological findings agree with the previously reported data in the literature containing the constituent of normal skin (Fig. 13) [39]. However, Masson trichrome stained skin of *Candida albicans* infected control rat reveals erosion or ulceration of the epidermis, edematous dermis and increased dermal vascularities. Also complete loss of the hair follicles with apparent sweat glands is observed (Fig. 14). Masson trichrome and Haematoxylin stained skin sections of rat infected with *Candida albicans* and treated with the available drug solution and Nystatin[®] cream (Figs. 15 and 16) reveal a smaller area of skin erosion, minimal ulceration and no characteristic hair follicles.

The *Candida albicans* infected skin and treated with the prepared formula NLC27 revealed areas of ulceration or incomplete loss of epidermis. Minimal polymorph leucocyte infiltration was evident. Laminated keratin was noticed. Also, minimal primitive hair follicles and many sebaceous glands were detected in the subepidermal area (Fig. 17). However, the skin of the group of rats infected with *Candida albicans* and treated with NLC3 revealed impressive improvement. No skin ulceration was detected in the examined sections (Fig.18). The recuperation of skin characteristic constituent was noticed in some sections, with the formation of primitive hair follicles and appearance of fully developed one. Also mild polymorphnuclear leucocytes in the subepidermal region were evident.

This improvement may be related to the better diffusion of the small sized particles of this formula in comparison to the other tested formulae. This suggestion is supported by the finding of Shuaidong et al. who proved that the smaller sized nanoparticles maximize their effective accumulation in tumor tissue [40]. Also similar results were obtained by Melkoumov et al. who found that Nyst nanosuspension has a higher antifungal effect on the *Candida albicans* compared to Nyst suspension [6].

The results obtained in this study prove that formula NLC3 can be employed as promising topical formulation for the treatment of skin fungal infection and can be subjected to further clinical studies after following the ethical applied steps.

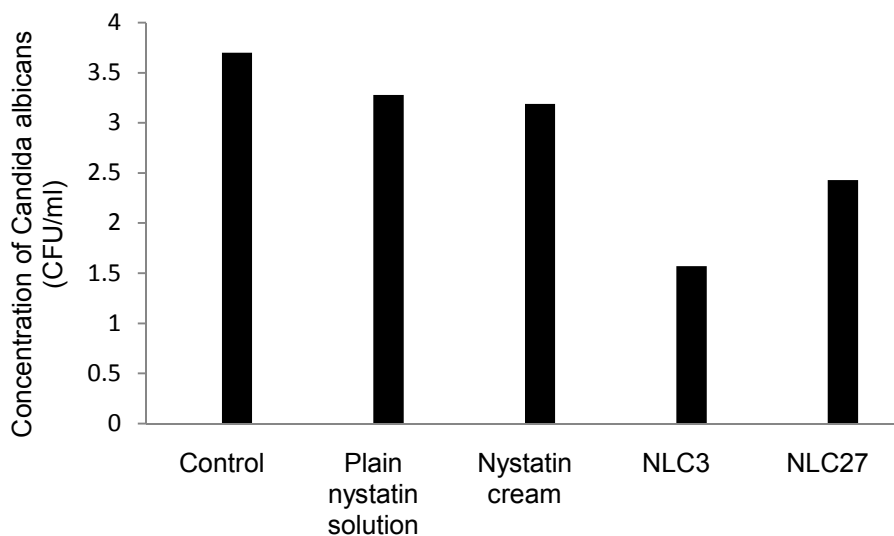


Fig. 12. Antifungal efficacy of Nystatin formulations expressed as colony forming unit (CFU) after treatment.

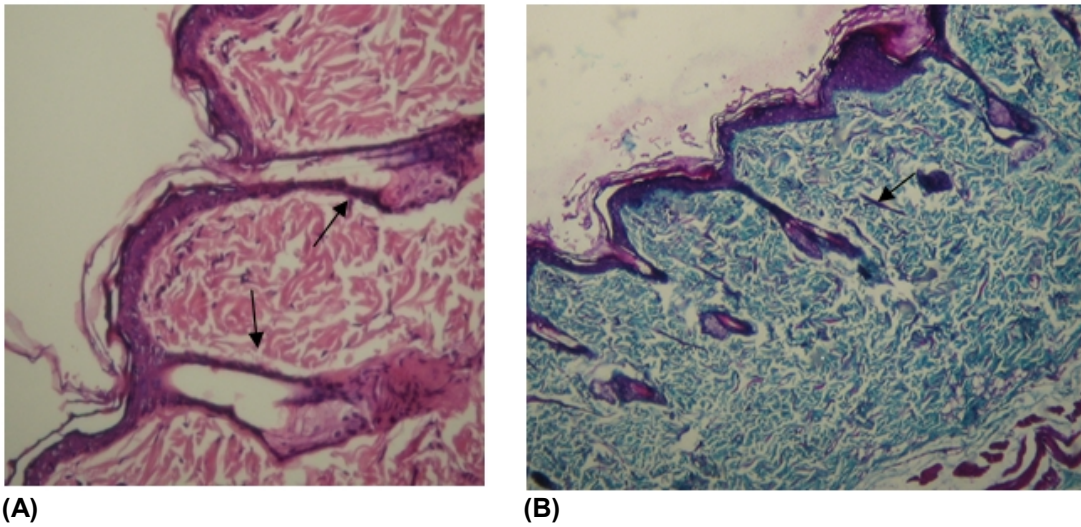


Fig. 13. (A) and (B) show normal skin stained with Hamatoxylin & eosin and Masson Trichrome respectively. Both sections reveal intact keratinized epidermis. The hair follicles (arrow) extend from the epidermis down into the dermis. Notice the thick dermal layer.

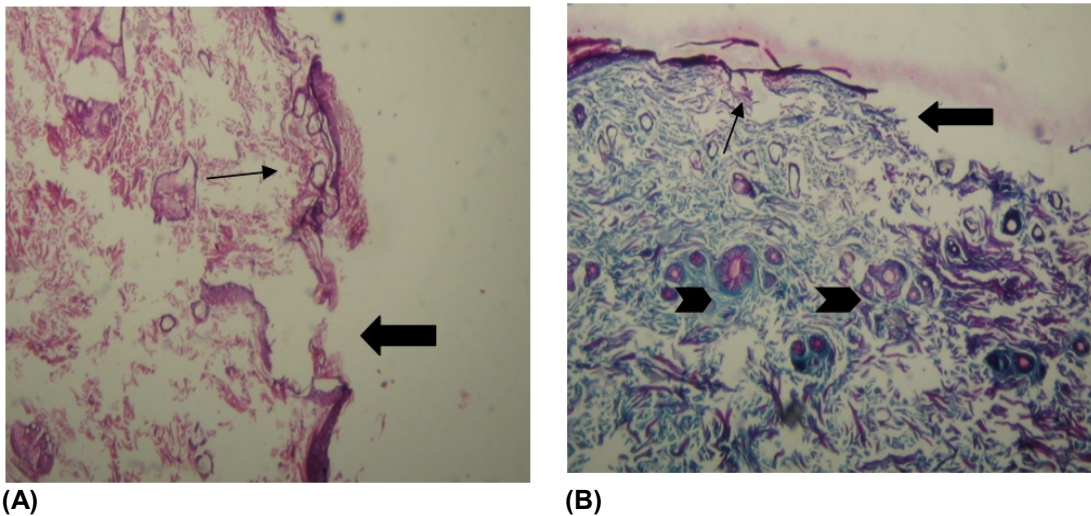


Fig. 14. Haematoxylin & eosin (A) and Masson trichrome (B) stained skin sections from control rat infected with *Candida albicans* reveal discontinuous ulcerated epidermis (thick arrow) in the vicinity of incomplete loss of other part or erosion. Many new vessels formation are disclosed in the upper part of the dermis (thin arrows). Note the absence of hair follicles and increased sweat glands (head of arrow) in the dermis. (x100).

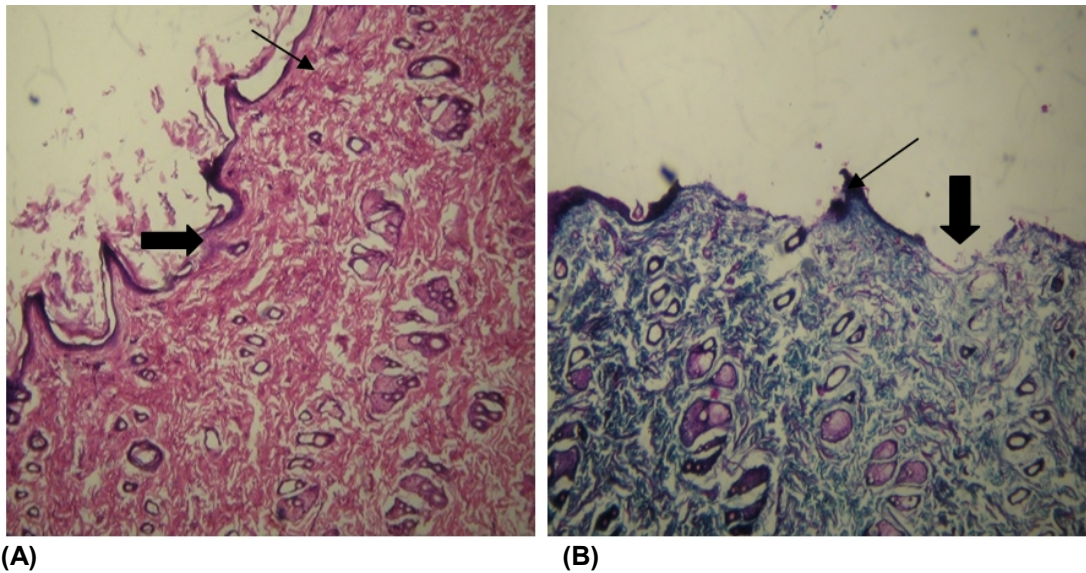


Fig. 15. Photomicrographs showing sections of rats skin treated with plain drug solution, (A) section stained with Haematoxylin and Eosin, (B) section stained with Masson trichrome. The sections reveal area of skin erosion (arrow), minimal ulceration (thick arrow) and no characteristic hair follicles.

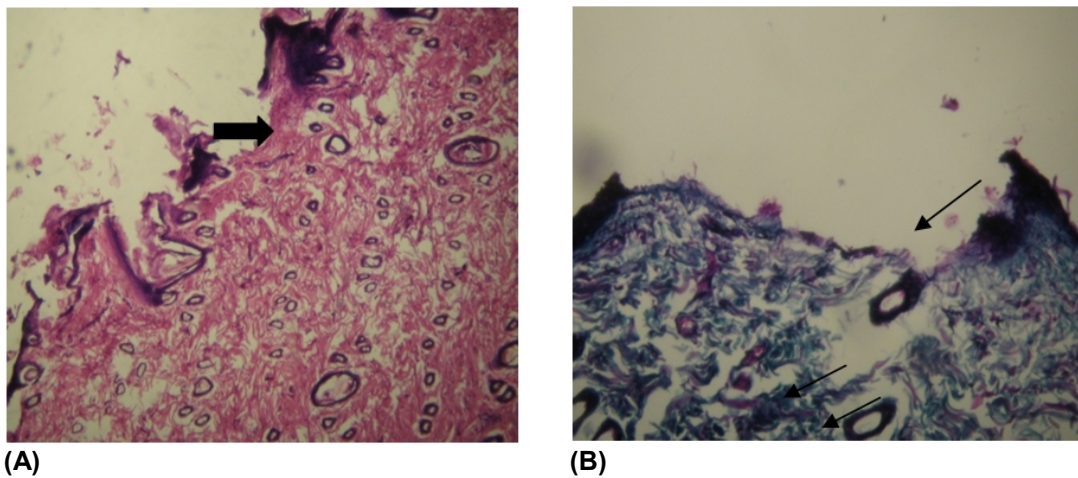


Fig. 16. Photomicrographs showing sections of rats skin treated with Nystatin[®] cream, (A) section stained with Haematoxylin and Eosin, (B) section stained with Masson trichrome. The sections reveal area of skin erosion (arrow), minimal ulceration (thick arrow) and no characteristic hair follicles.

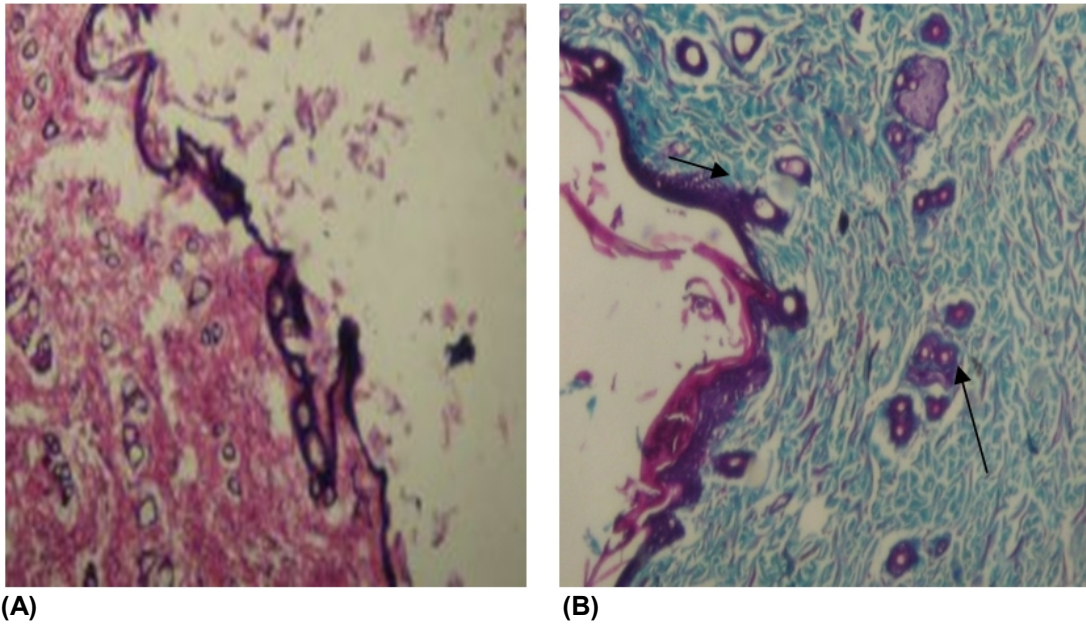


Fig. 17. Photomicrographs showing sections of rat skin treated with Nyst-NLC27,(A) & (B) sections stained with Haematoxylin and Masson trichrome. Sections reveal discontinuity of the skin. The intact epidermis (B) shows laminated keratin or stratum corneum. Note the sebaceous glands in the dermis and the primitive hair follicle formation (thin arrow).

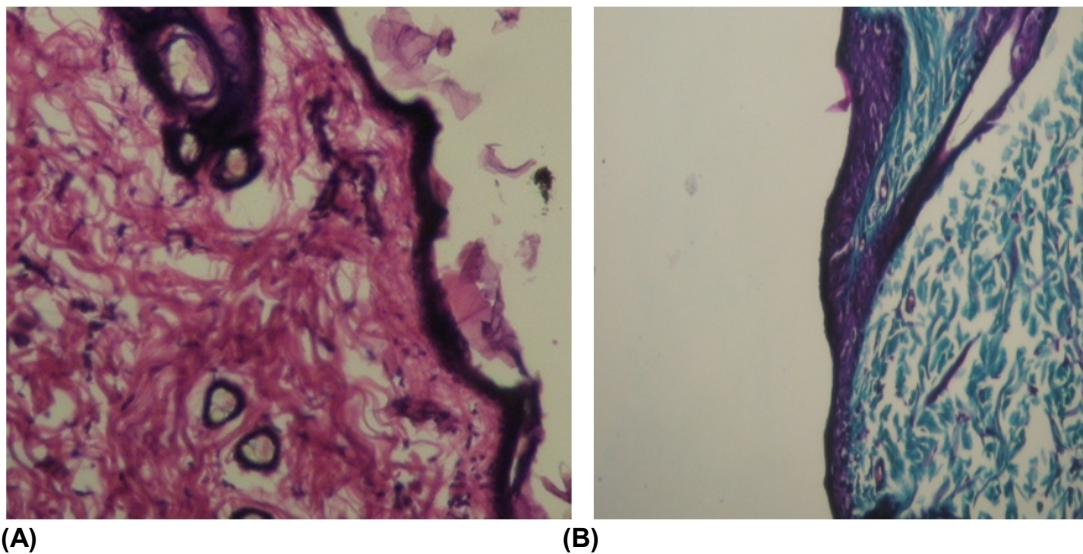


Fig. 18. Photomicrographs showing sections of the rat skin treated with Nyst-NLC3,(A) section stained with Haematoxylin and Eosin, (B) section stained with Masson trichrome. Improvement of the lesion with reformed skin layer evident in section (B) . Also in these sections primitive or well formed hair follicles are seen.

4. CONCLUSION

Homogenization followed by ultrasonication method is suitable to produce Nyst-NLCs. The lipophilic drug, Nyst, can be loaded in compritol using poloxamer 188 or PVA as surfactants and Miglyol 812 or Squalene as liquid lipids. The loading of nystatin proved to follow the drug-enriched-shell theory. DSC analysis showed amorphous state of Nyst. Nystatin is released more quickly when used in lower concentration. Stability studies proved that the 2 formulae suggested NLC3 and NLC27 are stable upon storage. Nyst-NLC3 formula tested for antifungal activity showed better results compared to the drug solution and the Nystatin[®] cream present in the market.

COMPETING INTERESTS

Authors have declared that no competing interests exist.

REFERENCES

1. Muller RH, Mader K, Gohla S. Solid lipid nanoparticles (SLN) for controlled drug delivery- A review of the state of the art. *Eur J Pharm Biopharm.* 2000;50:161-177.
2. Mehnert W, Mader K. Solid lipid nanoparticles: production, characterization and application. *Adv. Drug Deliv. Rev.* 2001;47:165-196.
3. Muller RH, Radtke M, Wissing SA. Solid lipid nanoparticles (SLN) and nanostructured lipid carriers (NLC) in cosmetic and dermatological preparations. *Adv. Drug Deliv. Rev.* 2002;1:131-55.
4. Radtke M, Souto EB, Muller RH. Nanostructured lipid carriers: a novel generation of solid lipid drug carriers. *Pharm. Technol. Eur.* 2005;17:45-50.
5. Quinones D, Evone MS, Ghaly S. Formulation and characterization of nystatin gel. – *PRHSJ.* 2008;27:62.
6. Melkoumov A, Goupil M, Louhichi F, Raymond M, Repentigny L, Leclair G. Nystatin nanosizing enhances in vitro and in vivo antifungal activity against *Candida albicans*. *J Antimicrob Chemother.* 2013;68(9):2099-105.
7. Manteiro DR, Silva S, Negri M, Gorup LF, de Camargo ER, Oliveira R, Barbosa DB and Henriques M, Antifungal activity of silver nanoparticles in combination with nystatin and chlorhexidine digluconate against *Candida albicans* and *Candida glabrata* biofilms. *Mycoses,* 2013;56:672-680.
8. Silva S, Pires P, Monteiro DR, Negri M, Gorup LF, de Camargo ER, Oliveira R, Williams DW, Henriques M, Azerdo J. The effect of silver nanoparticles and nystatin on mixed biofilms of *Candida glabrata* and *Candida albicans* on acrylic.
9. Sandri G, Bonferoni MC, Gokce EH, Ferrari F, Rossi S, Patrini M, Caramella C. Chitosan associated SLN: in vitro and ex vivo characterization of cyclosporine A loaded ophthalmic systems. *J Of Microencapsulation.* 2010;27:735-746.
10. Sharma A, Jindal M, Aggarwal G, Jain S. Development of a novel method for fabrication of solid lipid nanoparticles: using high shear homogenization and ultrasonication. *RJPBCS.* 2010;1:266.
11. Ekambaram PA, Abdul Hassan Sathali K, Priyanka. Solid lipid nanoparticles: A review. *Scientific Reviews & Chemical Communications.* 2012;2:82-85.
12. Gohla SH, Dingler A. Scaling up feasibility of the production of solid lipid nanoparticles (SLN). *Pharmazie.* 2001;56:61-63.

13. Souto EB, Wissing SA, Barbosa CM, Muller RH. Development of a controlled release formulation based on SLN and NLC for topical clotrimazole delivery. *Int J Pharm.* 2004;278:71.
14. Jifu H, Xinsheng F, Yanfang Z, Jianzhu W, Fengguang G, Fei L, Xinsheng P. Development and optimization of solid lipid nanoparticle formulation for ophthalmic delivery of chloramphenicol using a Box-Behnken design. *International journal of nanomedicine.* 2011;6:683-692.
15. Yang SC, Lu LF, Cai Y, Zhu JB, Liang BW, Yang CZ. Body distribution in mice of intravenously injected camptothecin solid lipid nanoparticles and targeting effect on brain. *J Control Release.* 1999;59:299.
16. Esposito E, Bortolotti F, Menegatti E, Cortesi R. Amphiphilic association systems for amphoterecin B delivery. *Int J Pharm.* 2003;260:249-260.
17. Ferrer J. Vaginal candidosis: epidemiological and etiological factors. *Int J Gynaecol Obstet.* 2000;71:21-27.
18. Wells JI. *Pharmaceutical formulations: The physicochemical properties of drug substances.* England: Ellis Horwood, Chichester; 1988.
19. Maebashi K, Toyama T, Uchida K, Yamaguchi H. A novel model of cutaneous candidiasis produced in prednisolone treated guinea pigs. *J Med Vet Mycol.* 1995;19:390-392.
20. Masson P. Some histological methods. Trichrome staining and their preliminary technique. *Bulletin of the International Association of Medicine.* 1929;12:75.
21. Puglia C, Blasi P, Rizza L, Schoubben A, Bonina F, Rossi C, Ricci M. Lipid nanoparticles for prolonged topical delivery: an in vitro and in vivo investigation. *Int. J. Pharm.* 2008;357:295-304.
22. Patlolla RR, Chougule M, Patel AR, Jackson T, Tata PNV, Singh M. Formulation, characterization and pulmonary deposition of nebulized celecoxib encapsulated nanostructured lipid carriers. *J. Control. Release.* 2010;144:233-241.
23. Chen CC, Tsai TH, Huang ZR, Fang JY. Effects of lipophilic emulsifiers on the oral administration of lovastatin from nanostructured lipid carriers: Physicochemical characterization and pharmacokinetics. *Eur. J. Pharm. Biopharm.* 2010;74:474-482.
24. Khalil RM, Abd El-Bary A, Kassem MA, Ghorab MM, Basha M. Nanostructured lipid carriers (NLCs) versus solid lipid nanoparticles (SLNs) for topical delivery of meloxicam. *Pharm. Dev. Technol;* 2013.
Available: <http://informahealthcare.com/phd>
25. Das, S., Ng, W.K., Tan, RBH. Are nanostructured lipid carriers (NLCs) better than solid lipid nanoparticles (SLNs): Development, characterizations and comparative evaluations of clotrimazole-loaded SLNs and NLCs? *Europ J Pharm Sci.* 2012;47:139-151.
26. Ekambaram P, Hasan SA. Formulation and evaluation of solid lipid nanoparticles of ramipril. *J Young Pharm.* 2001;3:216-220.
27. Abdelbary G, Fahmy RH. Diazepam loaded solid lipid nanoparticles: design and characterization. *AAPS Pharm Sci Tech.* 2009;10:215.
28. Radtke M, Souto EB, Muller RH. Nanostructured lipid carriers: a novel generation of solid lipid drug carriers. *Pharm. Technol. Eur.* 2005;17:45-50.
29. Patel D, Dasgupta S, Dey S, Ramani YR, Ray S, Mazumder B. Nanostructured lipid carriers (NLC)- based gel for the topical delivery of aceclofenac: Preparation, characterization and in vivo evaluation. *Scientia Pharmaceutica.* 2012;80:749-764.
30. Sheikh FA, Barakat NAM, Kanjwal MA, Aryal S, Khil MS, Kim HY. Novel self-assembled amphiphilic poly (ϵ -caprolactone)-grafted poly (vinyl alcohol) nanoparticles: hydrophobic and hydrophilic drugs carrier nanoparticles. *J. Master Sci. Mater Med.* 2009;20:821-831.

31. Fang JY, Fang CL, Liu CH, Su YH. Lipid nanoparticles as vehicles for topical psoralen delivery: solid lipid nanoparticles (SLN) versus nanostructured lipid carriers (NLC). *Eur. J. Pharm. Biopharm.* 2008;70:633-640.
32. Yuan H, Chen J, Du YZ, Hu FQ, Zeng S, Zhao HL. Studies on oral absorption of stearic acid SLN by a novel fluorometric method. *Colloids Surf. B.: Biointerfaces.* 2007;58:157-164.
33. Heiati H, Tawashi R, Shivers RR. Solid lipid nanoparticles as drug carriers I. Incorporation and retention of the lipophilic prodrug 3'-azido-3'-deoxythymidine palmitate. *Int. J. Pharm.* 1997;146:123-31.
34. Muller RH, Radtke M, Wissing SA. Solid lipid nanoparticles (SLN) and nanostructured lipid carriers (NLC) in cosmetic and dermatological preparations. *Adv. Drug Deliv. Rev.* 2002;1:131-55.
35. Higuchi WI. Analysis of data on the medicament release from ointments. *J. Pharm. Sci.* 1962;51:802-804.
36. Fang JY, Fang CL, Liu CH, SU YH. Lipid nanoparticles as vehicles for topical psoralen delivery: solid lipid nanoparticles (SLN) versus nanostructured lipid carriers (NLC). *Eur J Pharm Biopharm.* 2008;70:633-640.
37. Sivaramakrishnan R, Nakamura C, Mehnert W, Korting HC, Kramer KD, Schafer-Korting M. Glucocorticoid entrapment into lipid carriers-characterization by preelectric spectroscopy and influence on dermal uptake. *J Control Release.* 2004;97:493-502.
38. Gupta M, Vyas SP, Development, characterization and in vivo assessment of effective lipidic nanoparticles for dermal delivery of fluconazole against cutaneous candidiasis. *Chemistry and Physics of Lipids.* 2012;165:460.
39. Amany MM. Histological and immunohistochemical study on the effect of tretinoin on the skin of adult male albino rat. *Egypt. J. Histol.* 2008;31:208-219.
40. Shuaidong H, Huili M, Keyang H, Juan L, Tuo W, Shubin J, Jinchao Z, Shengtai H, Xing-jie L. Superior penetration and retention behavior of 50 nm gold nanoparticles in tumors. *Cancer Res.* 2012;73:1-12.

© 2014 Rawia et al.; This is an Open Access article distributed under the terms of the Creative Commons Attribution License (<http://creativecommons.org/licenses/by/3.0>), which permits unrestricted use, distribution, and reproduction in any medium, provided the original work is properly cited.

Peer-review history:

The peer review history for this paper can be accessed here:

<http://www.sciencedomain.org/review-history.php?iid=374&id=14&aid=2834>